Available online at www.sciencedirect.com
SCIENCE DIRECT®
ELSEVIER
Human Movement Science 22 (2003) 137–152
HUMAN MOVEMENT SCIENCE
www.elsevier.com/locate/humov

Eye–hand coupling during closed-loop drawing: Evidence of shared motor planning?

G. Anthony Reina *, Andrew B. Schwartz

The Neurosciences Institute, 10640 John Jay Hopkins Drive, San Diego, CA 92121, USA

Abstract

Previous paradigms have used reaching movements to study coupling of eye–hand kinematics. In the present study, we investigated eye–hand kinematics as curved trajectories were drawn at normal speeds. Eye and hand movements were tracked as a monkey traced ellipses and circles with the hand in free space while viewing the hand's position on a computer monitor. The results demonstrate that the movement of the hand was smooth and obeyed the 2/3 power law. Eye position, however, was restricted to 2–3 clusters along the hand's trajectory and fixed approximately 80% of the time in one of these clusters. The eye remained stationary as the hand moved away from the fixation for up to 200 ms and saccaded ahead of the hand position to the next fixation along the trajectory. The movement from one fixation cluster to another consistently occurred just after the tangential hand velocity had reached a local minimum, but before the next segment of the hand's trajectory began. The next fixation point was close to an area of high curvature along the hand's trajectory even though the hand had not reached that point along the path. A visuo-motor illusion of hand movement demonstrated that the eye movement was influenced by hand movement and not simply by visual input. During the task, neural activity of pre-motor cortex (area F4) was recorded using extracellular electrodes and used to construct a population vector of the hand's trajectory. The results suggest that the saccade onset is correlated in time with maximum curvature in the population vector trajectory for the hand movement. We hypothesize that eye and arm movements may have common, or shared, information in forming their motor plans.

* Corresponding author. Address: University of Pittsburgh, The McGowan Center Room 245 Pittsburgh, PA 15203, USA. Tel.: +1-858-626-2132/+1-412-383-6691; fax: +1-858-626-2199/+1-412-383-6799.

E-mail address: gar8+@pitt.edu (G.A. Reina).

0167-9457/03/$ - see front matter
doi:10.1016/S0167-9457(02)00156-2

PsycINFO classification: 2330; 2221; 2530
Keywords: Arm kinematics; Eye kinematics; Eye–hand coupling; 2/3 power law; Trajectory segmentation; Motor planning

1. Introduction

There have been many studies of eye and hand kinematics, however many studies focus on the two separately (de'Sperati & Viviani, 1997; Viviani & Terzuolo, 1982) or focus on eye movements tracking a previously recorded hand trajectory (Viviani, Campadelli, & Mounoud, 1987). These studies have demonstrated that hand movement (Viviani & Terzuolo, 1982) and smooth-pursuit eye movement (de'Sperati & Viviani, 1997) seem to be planned in "segments" of the overall trajectory. Points within the trajectory where the angular acceleration reaches local maxima delimit segments boundaries. Within each segment the hand or eye obeys a relationship between speed and curvature known as the 2/3 power law: the hand slows down on the curves and speeds up on the straightways (Eq. (1)).

$$\omega(t) = \kappa C(t)^{2/3} \tag{1}$$

where $\omega(t)$ is the angular velocity of the hand or eye, κ is the velocity gain factor (which changes between segments of the trajectory), $C(t)$ is the curvature of the path.

In these previous studies, eye movements were considered to be the focus of the task. In natural settings, however, eye and hand movements are typically coordinated such that the hand achieves a particular goal. It is unknown whether trajectory segmentation and the 2/3 power law will be reflected in eye movements when the handpath is the primary focus of the task.

Of those studies that have looked at eye–hand coupling, most have concentrated on reaching movements (Fischer & Rogal, 1986; Helsen, Elliott, Starkes, & Ricker, 1998; Neggers & Bekkering, 2000, 2001; Vercher, Gauthier, Cole, & Blouin, 1997). The eye typically saccades to the target before the hand and remains fixated on the target until the hand catches up. Typically, the eye has reached the target just as the arm movement reaches its peak velocity (Helsen et al., 1998). Interestingly, if the target is displaced well before the hand reaches its peak velocity, the subject can correct for the displacement accurately without any conscious perception of either the displacement or the correction (Goodale, Pelisson, & Prablanc, 1986). However, if a second target is presented after the hand has reached its peak velocity, the eye cannot saccade to that target until the hand has reached the initial target ("gaze anchoring;" Neggers & Bekkering, 2000). This suggests that eye and hand kinematics are not independent, but rather truly coupled movements whose relationship can evolve over the course of the task.

Only a few studies have looked at eye–hand coupling in more complex trajectories, such as curved paths (Gauthier & Mussa-Ivaldi, 1988; Vercher & Gauthier, 1992; Vercher et al., 1997). A curved-path would be essential to demonstrate the effect of the 2/3 power law in eye–hand coupling. In these previous studies, the subject was forced to trace the handpath at sub-normal speeds in order to obtain smooth pursuit eye movements following the hand's trajectory (0.3 cycles/s, Vercher et al., 1997; 0.2 and 0.5 cycle/s, Vercher & Gauthier, 1992; 0.5 cycle/s, Gauthier & Mussa-Ivaldi, 1988). In normal behavior, however, the subject does not typically make smooth pursuit eye movements that follow the hand precisely, but rather uses saccadic eye movements to move within and between complex motor tasks (Land & Hayhoe, 2001).

In the present study, we describe the kinematics of the hand and eye while the hand traced curved figures at normal speeds (>1 cycle/s; 0.2–0.5 m/s). We suggest that this test is a more natural paradigm for probing the features of eye–hand coupling because the behavioral constraints of the task are placed on hand movement and not on eye movement. We further ask if a visuo-motor illusion of hand movement – in which the visual input remains constant, but the hand trajectory does not – will alter eye movement. Using this illusion, we will test the hypothesis of whether hand and eye movements result from independent motor plans (no effect from the illusion on eye movements) or a common, coordinated plan (some effect from the illusion on eye movements).

2. Methods

2.1. Virtual reality simulator

A rhesus monkey (*Macaca mulatta*, 6 kg) was operantly trained to draw closed figures in a virtual reality simulator (Fig. 1). The behavioral setup has been described in detail elsewhere (Reina, Moran, & Schwartz, 2001). Briefly, the monkey sat in a primate chair with its head fixed. A custom-made stereo monitor was mounted in front of and above the monkey's head with the screen's display directed downward onto a mirror. The monkey viewed the reflected display through a stereoscopic shutter (Perceiva NuVision, McNaughton Industries) to produce an illusion of depth to the figure. A camera was used to record eye movements (point of gaze) at a sampling rate of 120 Hz (Model 501, Applied Science Labs).

An infrared marker was placed on the dorsum of the monkey's hand. The 3D position of the marker was measured in realtime by an optoelectronic tracking system (Optotrak 3020, Northern Digital). A computer (Indigo2, Silicon Graphics) recorded the current position of the monkey's hand and rendered a virtual representation of it to the stereo display. At all times during the experiment the monkey could see a sphere ("cursor" of radius 15 mm) in the virtual environment move with the same direction and speed as its hand. When in the simulator, the monkey could not see its hand or arm – only the virtual representation of hand location. The monkey received liquid rewards for performing the task correctly. In all cases, the monkey was treated in accordance with the Institutional Animal Care and Usage Committee and Society for Neuroscience guidelines.

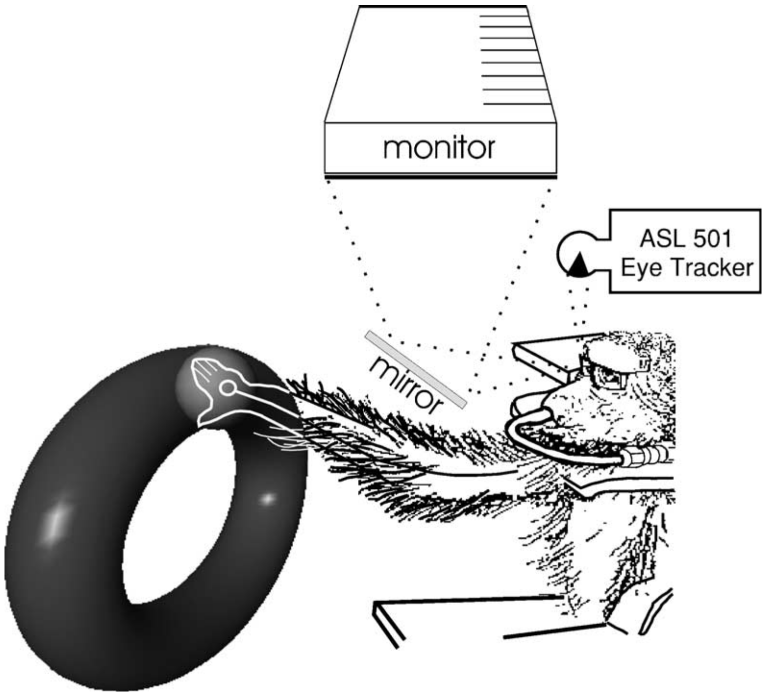

Fig. 1. Virtual reality setup – the monkey is seated and views the 3D image on the computer monitor as it is projected onto the mirror in front of him. An Optotrak marker on the hand causes a sphere on the monitor to move with the same velocity providing vision to the monkey of an otherwise obscured hand. Along with the sphere representing the hand, the template to trace (ellipse, circle) is projected on the monitor in 3D and is seen by the monkey on the mirror. An ASL 501 video eye tracker monitored the 2D position of the left eye.

2.2. Eye tracker calibration

To calibrate the eye tracker, a sphere ("target") was projected on the display in one of nine positions formed by a 3×3 square grid (24 cm on a side) that covered the display. The monkey was required to move the cursor sphere to the target sphere and hold it there for a random interval of 100–400 ms. With cursor and target sphere radii of 10 mm or smaller, the monkey would naturally foveate on the target sphere in order to accomplish the task. The target in the center of the display provided the calibration offset and the voltage change between targets provided the scaling factor of the eye tracker voltage to the distance on the screen.

2.3. Closed-loop tracing

The task began when the monkey touched the cursor to another target sphere positioned at the top of the virtual scene. After a random minimum hold time (300–500 ms), the target sphere disappeared and a template tube appeared which outlined the required trajectory (Fig. 1). The tube had a diameter of 30 mm and was either shaped as a circle (diameter of 100 mm) or an ellipse (major axis = 180 mm; minor axis = 100 mm). The monkey traced the path, keeping the cursor sphere in contact with the template tube. A reward was given for completing five cycles of the figure within 15 s. If the cursor moved outside of the template for more than 400 ms, then the trial was aborted. No upper limit was placed on how fast the monkey could trace the figure. A new trial could begin after an inter-trial interval (500–1000 ms). The ellipses and circles were drawn in blocks of five trials each.

2.4. Visuo-motor illusion tracing

In addition to drawing ellipses and circles, the monkey performed a task in which the actual handpath was different from the template displayed on the monitor. The first three cycles of the tracing were no different than the ellipse trial ("illusion off"). That is, the actual path of the hand followed the same trajectory as the figure displayed on the monitor (an ellipse). During the fourth cycle, the horizontal gain of hand excursion on the monitor was increased linearly in time from 1.0 to 1.8. For example, by the end of the fourth cycle, moving the hand 1 cm upward in space would move the cursor sphere 1 cm upward on the display, but moving 1 cm rightward in space would move the cursor sphere 1.8 cm rightward on the display. Because the ellipse template had a major/minor axis ratio of 1.8 in the horizontal direction, the monkey had to draw a circle with the hand in order to keep the cursor sphere within the template ("illusion on"). These trials were termed "exaggerated ellipse" because the visual feedback was an exaggerated motion of the hand's movement. The exaggerated ellipse was also drawn in blocks of 5 trials each.

2.5. Kinematic recording

The hand-position data were smoothed using a 10 Hz, low-pass, fifth-order, phase-symmetric digital filter (Woltring, 1986). The data for each of the five cycles were divided into 140 bins. Bin size was calculated by dividing the duration of the cycle by 100 equal intervals. Bin 50, for example, always represented the position of the hand when 50% of the path was completed. Twenty additional bins were assigned just prior to (pre-bins) and just after (post-bins) the cycle and had the same bin widths as the 100 movement bins.

Eye-position data were smoothed using the same digital filter as the hand marker but using a low-pass cutoff of 60 Hz. The eye-position data were divided into the same bins used for the hand-position data. Eye fixations were calculated using a modified version of a temporal–spatial clustering algorithm proposed by Helsen et al. (1998). A fixation was determined to have begun when the point of gaze had a standard deviation of less than 1° for 100 ms and would end when either the point of gaze deviated by at least 2° for 30 ms or at least 2.5° within 20 ms. Additionally, due to the closed-loop trajectory, if the first and last fixations overlapped within 2°, then the last fixation was considered to be part of the first fixation of the subsequent cycle.

2.6. Cortical recording

The electrophysiological methods and surgical procedures have been described previously in detail (Reina et al., 2001). After the monkey had been trained for several months in the task, a circular recording chamber (19 mm diameter) was placed over the contralateral pre-motor cortex under general anesthesia of isoflurane, ketamine, and xylazine. The recording chamber was stereotaxically targeted for placement just caudal to the genu of the arcuate sulcus and ventral to the spur (target = 18 mm anterior, 32 mm superior, 22 mm lateral from inter-aural origin). Extracellular recordings were made using glass-insulated, platinum–iridium electrodes (1–3 MΣ impedance) attached to a microdrive. Typically, only one penetration was made each day. Action potentials of single units were identified by the criteria of Mountcastle, Talbot, Sakata, and Hyvarinen (1969) and separated using a differential amplitude discriminator. Every attempt was made to record from all cortical layers. Recording sessions ranged from 4 to 6 h. The monkey was returned to its home cage after each session. Recordings from each hemisphere were performed over a six–eight week period.

2.7. Saccade-triggered average

To describe the temporal relationship between saccadic eye movements and smooth hand movements, we constructed a saccade-triggered average (STA). The STA is an average of the tangential hand velocity over a ± 200 ms window around a saccade in 10 ms intervals. The STA describes the temporal profile of the tangential hand velocity around the time of a saccade.

2.8. Population vector

A time series of population vectors based on instantaneous discharge rate in 8–9 ms bins was used to compare cortical population activity to the eye position by the STA described above.

$$\mathrm{PV}_{j,t} = \frac{1}{N}\sum_{i=1}^{N}\left(\frac{D^*_{i,t} - \hat{D}^*_i}{D^*_{i_{\max}} - \hat{D}^*_i}\,\frac{b_{i,j}}{\sqrt{\sum_{j=1}^{3} b^2_{i,j}}}\right) \tag{2}$$

where $\mathrm{PV}_{j,t}$ is the population vector for coordinate j at time bin t, $D^*_{i,t}$ is the discharge rate of cortical unit i at time t, $\hat{D}^*_i$ is the geometric mean of discharge rate of unit i over all cycles, $D^*_{i_{\max}}$ is the maximum discharge rate of unit i over all movements, $b_{i,j}$ is the regression coefficient for cortical unit i and coordinate j (x, y, or z direction), N is equal to the number of cortical units.

The regression coefficients ($b_{i,j}$), or preferred directions, in Eq. (1) were calculated from a reaching paradigm (center → out task) described in a previous paper (cf. Reina et al., 2001). The results of Eq. (2) were integrated in time to yield a population trajectory. A time lag was incorporated in the discharge rate of each unit based on the best correlation between the predicted and actual discharge rate.

3. Results

3.1. Kinematics of the hand

Data for 565 ellipse, 610 circle, and 511 exaggerated ellipse trials were collected from both arms of one monkey over a six week period. Each trial consisted of five cycles of the figure. The average hand trajectory for each cycle of the three trajectories is plotted in Fig. 2. The eccentricity (major/minor axis) of the average trajectory is 1.38 (SD 0.05) for the circle task (Fig. 2(a)) and 1.73 (SD 0.06) for the ellipse task (Fig. 2(b)). In Fig. 2(c), each cycle is denoted with a different marker. Note that the trajectory of the hand changes from an eccentricity of 1.72 (SD 0.04) (cycles 1–3, referred to as "illusion off") to 1.24 (cycle 5, referred to as "illusion on"). The visual display remained constant (i.e. an elliptical tube) for these cycles. A regression between the logarithms of tangential hand velocity and the radius of curvature confirmed that the kinematics of the hand obeyed the 2/3 power law (Ellipse: slope $=$ 0.327, $r^2 = 0.780$; circle: slope $= 0.319$, $r^2 = 0.701$; illusion on slope $= 0.319$, $r^2 =$ 0.528).

3.2. Kinematics of the eye

A review of the raw data indicated that the eye fixated on 2–3 regions of the trajectory (for an example, see Animation 1, http://dell2.neurobio.pitt.edu). The eye remained fixated on one of these regions 78.6% (SD 3.74) of the time and tended to saccade successively between the fixation regions. A polar histogram of the fixation angle of the eye highlights these fixation regions (0° and 195°; Fig. 3). Data from the third cycle of the ellipse, circle, and exaggerated ellipse tasks are plotted in Fig. 3(a–c). Data from the fifth cycle of the ellipse task are plotted in Fig. 3(d). Note that in this fifth cycle, it appears as if the cursor moving about an ellipse on the computer monitor, but the hand trajectory is actually more circular (i.e. illusion is "on"). A Kruskal–Wallis test on these four eye position distributions demonstrated that they were not equivalent ($\chi^2 = 15.62$; $p = 0.0014$). In pairwise comparisons of the distributions, the ellipse (3a) and exaggerated ellipse with the illusion off (3c) were significantly different than the circle (3b) distribution ($p < 0.05$ with Bonferroni correction). The exaggerated ellipse with the illusion on (3d) was not significantly different than any of the other distributions. This indicates that the eye position distribution for the exaggerated ellipse task shifted from the "ellipse" distribution toward the "circle" distribution as the illusion progressed.

A density plot, or 2D histogram, of the eye position data is plotted in Fig. 4 for the ellipse, exaggerated ellipse, and circle task (left to right columns). The last three rows (b–d) are density plots of hand position during one of three eye fixations. Fig. 4(a) shows a density plot of all eye positions during the third cycle of the ellipse and circle tasks (columns 1 and 3) and the fifth cycle of the exaggerated ellipse task (column 2). The density plot is constructed with 100 equally spaced bins from −100 to +100 mm of the center of the monitor's display. The color of each bin is proportional to the number of times the eye position falls within that bin (blue < red). There are

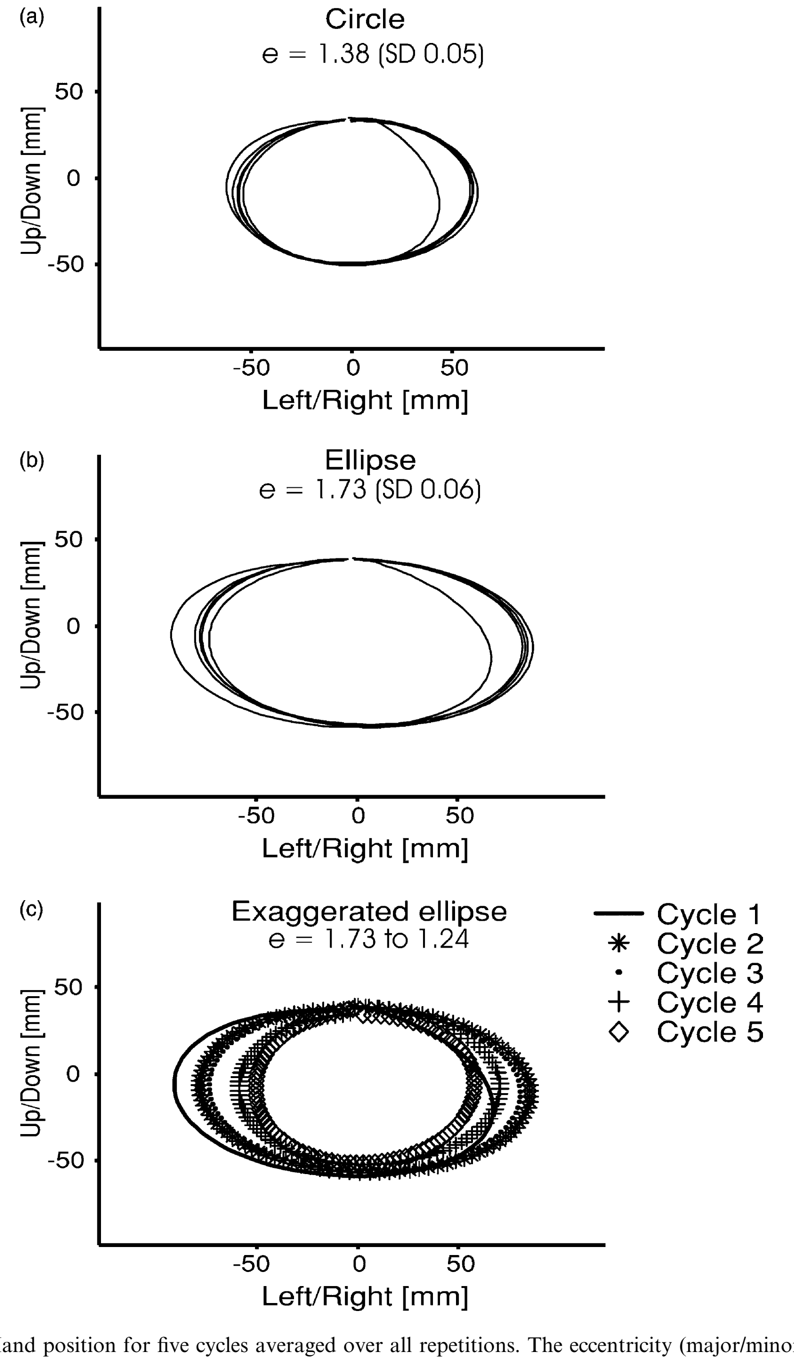

Fig. 2. Hand position for five cycles averaged over all repetitions. The eccentricity (major/minor axis) is listed for the circle (a), ellipse (b), and exaggerated ellipse (c) tasks. Note in the exaggerated ellipse (2c) that the average hand trajectory becomes more circular (1.73–1.24) between the third and fifth cycles.

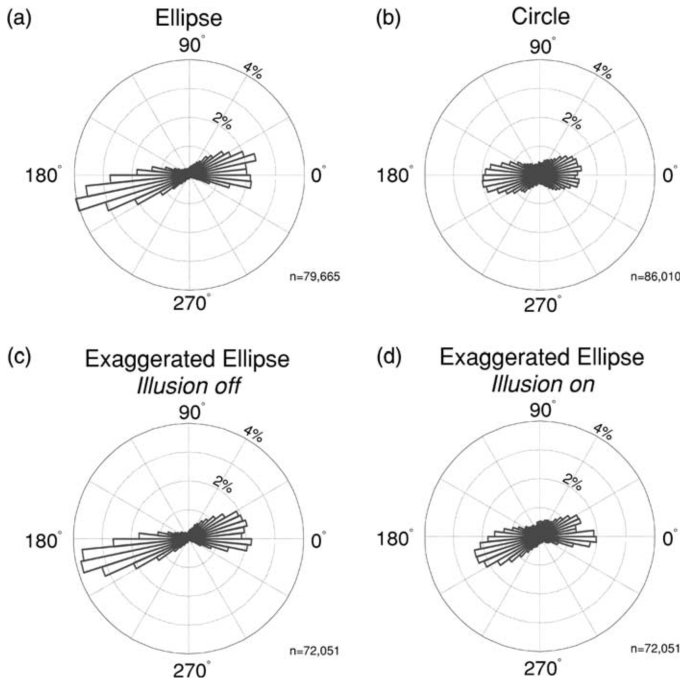

Fig. 3. Polar histograms of eye fixations for cycle 3 (a–c) or cycle 5 (d). A Kruskal–Wallis test confirmed that the "ellipse" (a) and "illusion off" (c) histograms are not statistically different, but are significantly different from the "circle" (b) histogram. The "illusion on" histogram is not statistically different from any of the others indicating that its distribution falls somewhere between that of the ellipse and circle.

2–3 distinct clusters of eye position in the ellipse and exaggerated ellipse tasks and three less distinct clusters in the circle task. In 4(b–d), we define a region of interest for each eye cluster (white dots) and superimpose a density plot of hand positions when the eye is fixated within that cluster. Fixations occurred spatially near places of high curvature in the hand trajectory. Fixation intervals begin approximately at a local maximum in tangential hand velocity and end just after a local minimum (i.e. the point of locally maximum curvature).

To better assess the temporal relationship between the fixation regions and hand-path characterization, we calculated a STA of the tangential velocity of the hand. The STA is the average tangential velocity profile of the hand and is centered at the end of a fixation period. The end of the fixation correlated with the beginning of a saccade for this task. In Fig. 5, the STA for the right (45°) and left (195°) fixations are plotted with their 95% confidence intervals. Notice that the end of the fixation consistently occurred as the hand was about to reach the maximum tangential velocity. This implies that the next fixation segment should be reached sometime during the straightest part of the trajectory (where the tangential velocity is at a local maximum and the segments change). The eye saccaded to the next fixation segment approximately 50–100 ms ahead of the hand. The eye reached that fixation before the

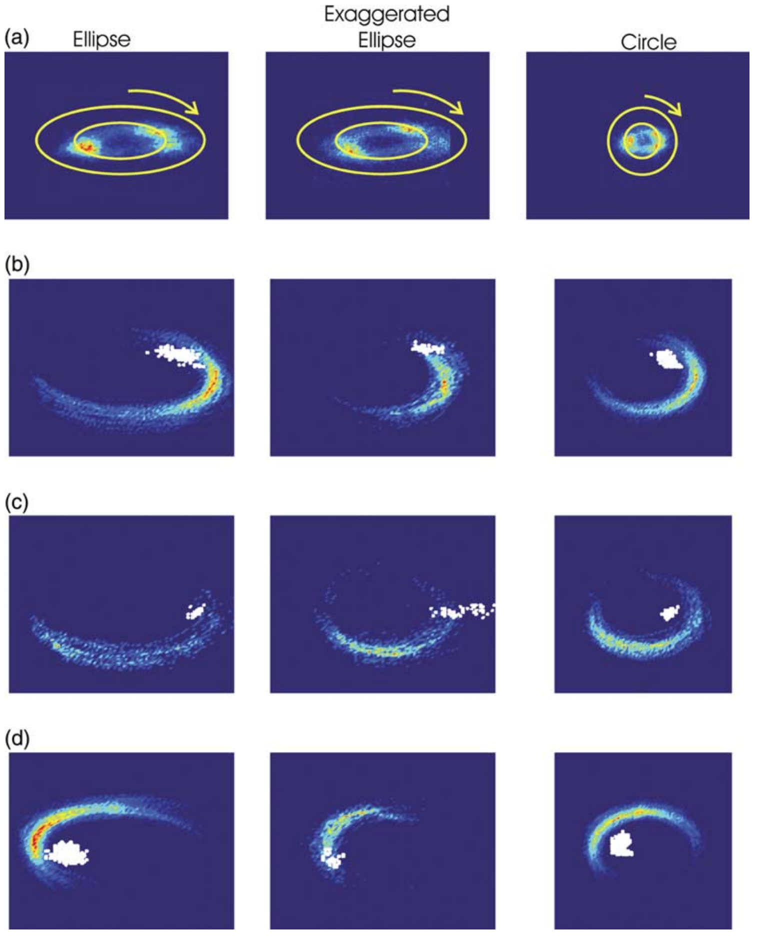

Fig. 4. The three columns are data from the ellipse, exaggerated ellipse, and circle tasks respectively. (a) A density plot of the eye positions for cycle 3 (ellipse and circle) or cycle 5 (exaggerated ellipse, illusion on). The traced figure is superimposed. The density plot is a 2D histogram with 100 equally spaced bins from −100 to +100 mm from the center of the monitor's display. The color of each bin is proportional to the number of times the eye position falls within that bin (blue < red). (b–d) The last three rows are density plots of hand position during one of the three eye fixation clusters (white overlay) found in the first row. For example, row (d) shows the hand positions for when the eye position was within the leftmost (195°) cluster of found in the eye density plot of row (a).

hand an average 27 ms (SD 13 ms) for the ellipse task, 25 ms (SD 14 ms) for the circle task, and 20 ms (SD 13 ms) for the "illusion on" task.

3.3. Population vector segmentation

In the final part of the analysis, population vectors trajectories of the handpath were constructed using Eq. (2). Post-mortem analysis confirmed that the cortical

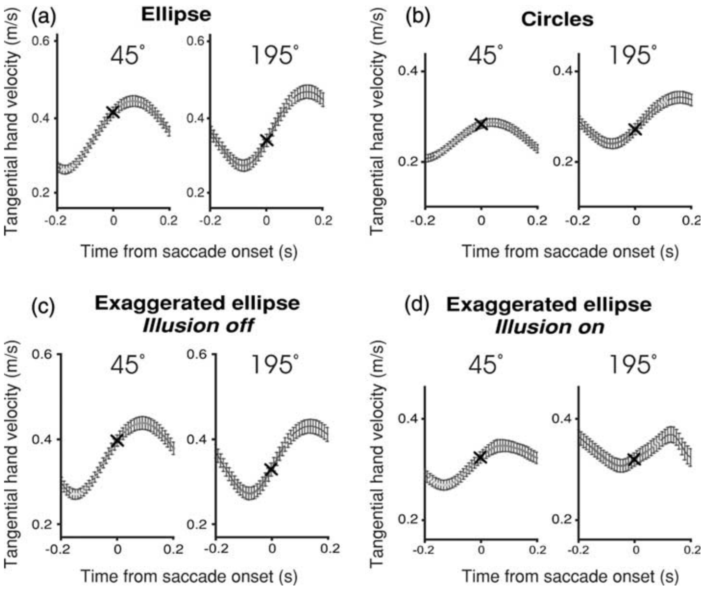

Fig. 5. A STA plot of tangential hand velocity. Whenever the eye left a fixation cluster, a ± 200 ms window was taken of the tangential hand velocity profile in a running average. The vertical bars are 95% CI and the 'X' denotes the onset of the saccade. Note that the saccade consistently occurs after the tangential velocity of the hand has reached a local minimum (maximum curvature in the trajectory) but before it reaches a local maximum (beginning of next segment in the trajectory).

units used in the population vector were from the ventral pre-motor area (F4). We found many cortical units that were modulated to visual stimuli and movement of the arm, which is typical of neurons of this cortical area.

There were 123 cortical units recorded with eye and hand kinematic data from both hemispheres of one monkey. Of those, 23 cortical units recorded during the circles task, 25 during the ellipse task, and 23 during the exaggerated ellipse task had statistically significant preferred directions in a 3D center → out task ($r^2 >= 0.83$) and were located in ventral pre-motor cortex. The instantaneous firing rates of these cortical units were shifted in time according to the best correlation between the actual and predicted instantaneous discharge rates and then used to create the population vector trajectory (Eq. (2)). Fig. 6(a) shows the average population vector trajectory during cycle 3 of the ellipse task (bin size = 9.2 ms). The STA of the neural population vector (Fig. 6(a)) is similar to and slightly leading that produced from the actual tangential hand velocity (Fig. 5(a)).

3.4. Vertical ellipse

One confound of the present experiment is that the monkey had performed the task repetitively. The fixation segments may result from the monkey learning that

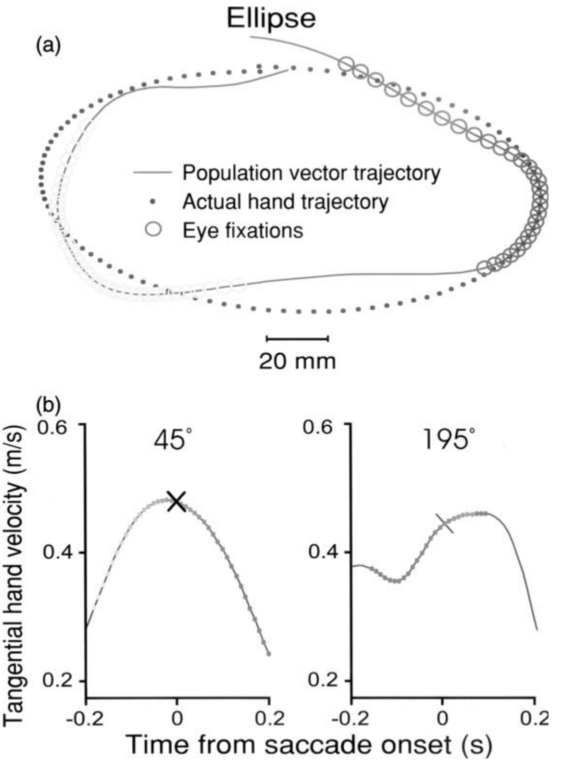

Fig. 6. (a) *Solid line*: Population vector trajectory from area PMv (bin size = 9.2 ms); *Closed circles*: Average hand trajectory; *Open circles*: Times in the trajectory where the eye was fixed (mean ±1 SD). (b) A STA plot for the population vector tangential velocity profile during the ellipse task. The saccade occurs closer to the maximum tangential velocity in the population vector trajectory than in the actual tangential velocity of the hand (compare with Fig. 5a). The maximum tangential velocity is the changepoint in the two segments of the trajectory.

the errors in handpath are greatest at the corners. While the present experiment could not rule out such an explanation, we asked whether the fixations would change if the ellipse were oriented vertically. Fig. 7 shows the eye position density plot and polar histogram for the vertical ellipses. As predicted, the fixation clusters rotated with the curvature. This pattern was evident within the first few repetitions of this novel task. We also re-tested the circle tracing after the vertical ellipse trials and found that there was no longer any obvious clustering of the eye's position. This would have been expected if the eye fixations were really set on regions of maximum curvature because a circle has a constant curvature and, therefore, no maximum region of curvature on which to fixate. However, although the visual image was the same circle for both trials, the hand's trajectory was more circular (major/minor axis = 1.10) for the re-tested circle tracing than for the original circle testing (major/minor axis = 1.38). The hand's trajectory may be an important factor in determining the fixation clusters on the visual image.

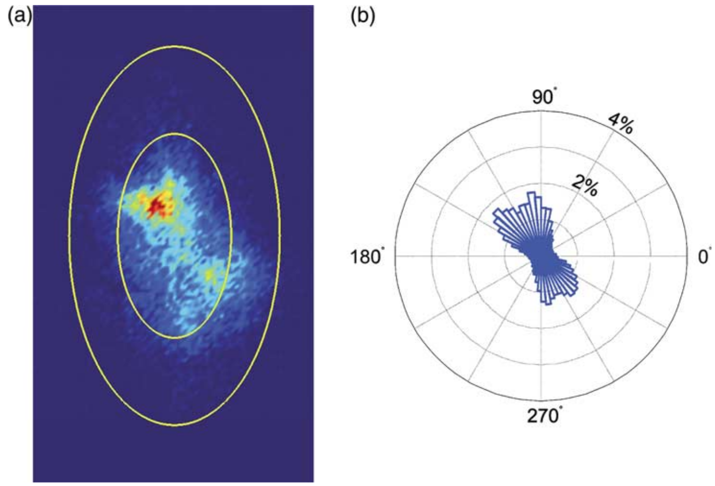

Fig. 7. Vertical ellipse. The monkey traced the ellipse rotated vertically. In the eye density (a) and eye position histogram (b) plots the eye fixation cluster rotated with the curvature.

4. Discussion

4.1. Kinematic coupling of the eye to the hand

Previous studies have investigated eye–hand coupling for slowly traced trajectories and found smooth pursuit eye movements that followed the trajectory of the hand (Gauthier & Mussa-Ivaldi, 1988; Gauthier, Vercher, Mussa-Ivaldi, & Marchetti, 1988; Vercher & Gauthier, 1992; Vercher et al., 1997). In contrast, our experiment found that, when drawing at normal speeds, eye movements were saccadic between fixation clusters anchored to the maximum curvature along the hand's trajectory. Further, fixations changed during an illusion in which the visual input remained constant but the arm movement varied. This would suggest that the saccades are planned with regard to the hand's trajectory. It concurs with Gielen, van den Heuvel, and van Gisbergen (1984) who suggested that separate mechanisms exist for the initiation of eye and arm movement but common mechanisms plan the end position of the movement.

More specifically, our results suggest that the eye planning was made assuming the handpath would be segmented in accordance with the 2/3 power law. Saccades consistently occurred just before the hand had moved into the subsequent segment of the path and fixated near the point of maximum curvature in the subsequent segment (where the tangential hand velocity is decelerating to a local minimum). This agrees with studies of eye–hand coordination during reaching that have shown the eye reaches the target by the time the hand is in the deceleration phase of the movement (Helsen et al., 1998). It is also consistent with the ‘‘gaze anchoring’’ seen when a second target is presented after the hand has reached its peak velocity

(Neggers & Bekkering, 2000, 2001). In effect, the eye is anchored to the maximum curvature within the upcoming segment of the trajectory until just before it has reached the next segment.

4.2. Motor memory or motor prediction?

The hand slows down near regions of high curvature presumably to ensure accurate tracing. Intuitively, such eye kinematics would aid the hand to accurately trace the required path by fixing the fovea on the points of highest curvature. However, there could be several explanations for the observed fixation.

One explanation is that over-training may allow the monkey to learn that the maximum curvature has a greater significance. That is, the monkey may chose to fixate on these areas of the display because the greater errors in handpath are likely to occur at the corners. The monkey, therefore, attends to the areas in the display where it is error-prone. In an attempt to test this explanation, we rotated the ellipse vertically and asked whether the fixation points rotated accordingly. They indeed rotated even with the first correct trial. Land and colleagues have shown that automobile drivers fixate on a similar point near the tangent of the road ahead regardless of whether they are familiar with the road (Land & Tatler, 2001) or not (Land & Lee, 1994). For example, Land and Lee (1994) demonstrated that while driving an automobile, humans invariably fixate the eyes near the point of maximum curvature along the road ahead approximately 1–2 s prior to reaching the curve and maintain their gaze relatively fixed to that point while negotiating the curve. In that experiment, no learning of the trajectory had taken place. Moreover, both naïve and experienced subjects were unaware of the prolonged fixations at the curves.

Is the attention represented by fixation anchored to a static, memorized position or determined in real-time by the progression of the task? In the latter case, the eye and arm movements share common information in their planning. It is interesting that the decision of where to make a saccade occurs within the previous segment of the trajectory. As noted in the STA of the population vector (Fig. 5(b)), the saccade occurs close to the local maximum of the population vector. If the population vector were a true representation of the neural activity governing the arm, then this might serve as a saccade trigger. Rather than the eyes fixating on areas of high curvature due to memorization, they may receive feedforward information about the upcoming arm movement. Ariff, Donchin, Sachs, and Shadmehr (2001) have demonstrated that eye movements use an efferent copy of the planned arm movement. Land and McLeod (2000) demonstrated that cricket batsmen saccade ahead of the approaching ball to the predicted point of contact based on the initial trajectory of the ball. Although the kinematics of the ball may be stereotypical, the actual trajectory of the ball could vary significantly between pitches. Simply memorizing points of interest along the average trajectory may not be an effective strategy to consistently hit the ball. Vercher et al. (1997) concluded that indeed there is a reciprocal exchange of information between eye and arm planning. Such a strategy would work even in the absence of vision.

4.3. Neural substrate

Evidence of coordinated arm and eye movement control has also been found in the superior colliculus (Stuphorn, Bauswein, & Hoffmann, 2000), dorsal pre-motor area (Boussaoud, Jouffrais, & Bremmer, 1998; Fujii, Mushiake, & Tanji, 2000), ventral pre-motor area (Mushiake, Tanatsugu, & Tanji, 1997), parietal reach regions (Batista, Buneo, Snyder, & Andersen, 1999), and the cerebellum (Vercher & Gauthier, 1988). Most of these studies conclude that eye movement influences arm movement. Conversely, Vercher and Gauthier (1988) suggested that arm movement could influence eye movement via feedback of arm kinesthetics within the dentate nucleus of the cerebellum. Our results suggest that eye movements may also be influenced by predictive information concerning the kinematics of the arm and reinforce the theory that trajectory segmentation and the 2/3 power law may be a product of neural motor planning.

References

Ariff, G. D., Donchin, O., Sachs, M. B., & Shadmehr, R. (2001). Saccades during reaching movement suggest a forward model of arm dynamics. *Society for Neuroscience Abstracts, 27*, 302.5.

Batista, A. P., Buneo, C. A., Snyder, L. H., & Andersen, R. A. (1999). Reach plans in eye-centered coordinates. *Science, 285*(5425), 257–260.

Boussaoud, D., Jouffrais, C., & Bremmer, F. (1998). Eye position effects on the neuronal activity of dorsal premotor cortex in the macaque monkey. *Journal of Neurophysiology, 80*(3), 1132–1150.

de'Sperati, C., & Viviani, P. (1997). The relationship between curvature and velocity in two-dimensional smooth pursuit eye movements. *Journal of Neuroscience, 17*(10), 3932–3945.

Fischer, B., & Rogal, L. (1986). Eye–hand-coordination in man: A reaction time study. *Biological Cybernetics, 55*(4), 253–261.

Fujii, N., Mushiake, H., & Tanji, J. (2000). Rostrocaudal distinction of the dorsal premotor area based on oculomotor involvement. *Journal of Neurophysiology, 83*(3), 1764–1769.

Gauthier, G. M., & Mussa-Ivaldi, F. (1988). Oculo-manual tracking of visual targets in monkey: Role of the arm afferent information in the control of arm and eye movements. *Experimental Brain Research, 73*(1), 138–154.

Gauthier, G. M., Vercher, J. L., Mussa-Ivaldi, F., & Marchetti, E. (1988). Oculo-manual tracking of visual targets: Control learning, coordination control and coordination model. *Experimental Brain Research, 73*(1), 127–137.

Gielen, C. C., van den Heuvel, P. J., & van Gisbergen, J. A. (1984). Coordination of fast eye and arm movements in a tracking task. *Experimental Brain Research, 56*(1), 154–161.

Goodale, M. A., Pelisson, D., & Prablanc, C. (1986). Large adjustments in visually guided reaching do not depend on vision of the hand or perception of target displacement. *Nature, 320*(6064), 748–750.

Helsen, W. F., Elliott, D., Starkes, J. L., & Ricker, K. L. (1998). Temporal and spatial coupling of point of gaze and hand movements in aiming. *Journal of Motor Behavior, 30*(3), 249–259.

Land, M. F., & Hayhoe, M. (2001). In what ways do eye movements contribute to everyday activities? *Vision Research, 41*(25–26), 3559–3565.

Land, M. F., & Lee, D. N. (1994). Where we look when we steer. *Nature, 369*(6483), 742–744.

Land, M. F., & McLeod, P. (2000). From eye movements to actions: How batsmen hit the ball. *Nature Neuroscience, 3*(12), 1340–1345.

Land, M. F., & Tatler, B. W. (2001). Steering with the head: the visual strategy of a racing driver. *Current Biology, 11*(15), 1215–1220.

Mountcastle, V. B., Talbot, W. H., Sakata, H., & Hyvarinen, J. (1969). Cortical neuronal mechanisms in flutter-vibration studied in unanesthetized monkeys. Neuronal periodicity and frequency discrimination. *Journal of Neurophysiology, 32*(3), 452–484.

Mushiake, H., Tanatsugu, Y., & Tanji, J. (1997). Neuronal activity in the ventral part of premotor cortex during target-reach movement is modulated by direction of gaze. *Journal of Neurophysiology, 78*(1), 567–571.

Neggers, S. F., & Bekkering, H. (2000). Ocular gaze is anchored to the target of an ongoing pointing movement. *Journal of Neurophysiology, 83*(2), 639–651.

Neggers, S. F., & Bekkering, H. (2001). Gaze anchoring to a pointing target is present during the entire pointing movement and is driven by a non-visual signal. *Journal of Neurophysiology, 86*(2), 961–970.

Reina, G. A., Moran, D. W., & Schwartz, A. B. (2001). On the relationship between joint angular velocity and motor cortical discharge during reaching. *Journal of Neurophysiology, 85*(6), 2576–2589.

Stuphorn, V., Bauswein, E., & Hoffmann, K. P. (2000). Neurons in the primate superior colliculus coding for arm movements in gaze-related coordinates. *Journal of Neurophysiology, 83*(3), 1283–1299.

Vercher, J. L., & Gauthier, G. M. (1988). Cerebellar involvement in the coordination control of the oculo-manual tracking system: Effects of cerebellar dentate nucleus lesion. *Experimental Brain Research, 73*(1), 155–166.

Vercher, J. L., & Gauthier, G. M. (1992). Oculo-manual coordination control: ocular and manual tracking of visual targets with delayed visual feedback of the hand motion. *Experimental Brain Research, 90*(3), 599–609.

Vercher, J. L., Gauthier, G. M., Cole, J., & Blouin, J. (1997). Role of arm proprioception in calibrating the arm–eye temporal coordination. *Neuroscience Letters, 237*(2–3), 109–112.

Viviani, P., Campadelli, P., & Mounoud, P. (1987). Visuo-manual pursuit tracking of human two-dimensional movements. *Journal of Experimental Psychology and Human Perceptual Performance, 13*, 62–78.

Viviani, P., & Terzuolo, C. (1982). Trajectory determines movement dynamics. *Neuroscience, 7*(2), 431–437.

Woltring, H. J. (1986). A Fortran package for generalized, cross-validatory spline smoothing and differentiation. *Advances in Engineering Software, 8*(2), 104–113.